A Revised Mid-Pliocene Composite Section Centered on the M2 Glacial Event for ODP Site 846

√Timothy D. Herbert[1], Rocio Caballero-Gill[1,2] and Joseph B. Novak[1,3]

[1]Department of Earth, Environmental and Planetary Sciences, Box 1846, Brown University, Providence RI 02906 U.S.A.

[2]Atmospheric, Oceanic, and Earth Sciences, George Mason University, University Dr., Fairfax VA 22030 U.S.A.

[3]University of California Santa Cruz, Santa Cruz, CA U.S.A.

Correspondence to: Timothy D. Herbert (timothy_herbert@brown.edu)

Manuscript date: October 21, 2019

Abstract

The composite section from ODP Site 846 has provided key data sets for Pliocene stable isotope and paleoclimatic time series. We document here apparent outliers in previously published data sets for stable isotopes and alkenone-derived sea surface temperature estimates (SST) in the late Pliocene interval containing the M2 glaciation (ca. 3.290-3.3 Ma) by tying high resolution core measurements to a continuous downhole conductivity log. We generate a revised sequence of new stable isotopic and alkenone measurements across the M2 event that correlate well to the revised splices of color reflectance and gamma ray attenuation porosity evaluator data from Site 846, and to a new composite section produced at equatorial Pacific ODP Site 850. A new composite splice for Site 846 is proposed, along with composite isotope and alkenone time series that should be integrated into revised Pliocene paleoclimatic stacks.

Keywords: Pliocene paleoceanography, stable isotopes, alkenone SST, Pliocene stratigraphy, hydraulic piston coring

1 Introduction

Continuous proxy time series from ODP Site 846 occupy a privileged place in Pliocene stratigraphy and paleoclimatology. Drilled during Leg 138, this site was one of the first to systematically integrate high resolution, non-destructive core scanning into the construction of composite sections (Shipboard Scientific Party, 1992; Hagelberg et al., 1995) that formed the basis for later detailed shore-based studies. The creation of composite sections was necessitated by the fact that coring does not completely recover the sequence at any one drill hole; continuous records must be stitched together to fill in coring gaps. Among the fruits of this work were some of the longest, best resolved time series of Pliocene stable isotopic variations (Shackleton et al., 1995b), lithological variations (Hagelberg et al., 1995) and tropical sea surface temperatures (Lawrence et al., 2006; Herbert et al., 2010) and a proposal for an orbitally-tuned late Neogene time scale (Shackleton, 1995a). The continuity and high sedimentation rate at site 846 resulted in its isotopic data set playing an outsized role in the Pliocene interval of the widely used LR04 isotopic stack (Lisiecki and Raymo, 2005. However, it was noted (Figure 9 of Lisiecki and Raymo, 2005) that the isotopic record in the interval surrounding the glacial event M2 (circa 3.3 Ma) at Site 846 is anomalous in comparison to other sites.

In this contribution we document significant errors in the late Pliocene (equivalent to the Gauss magnetochron) composite section at Site 846. These affect the stable isotopic and paleotemperature reconstructions around the Pliocene M2 isotopic event, the most notable Pliocene glacial stage preceding cyclic northern hemisphere glaciation at ~ 2.7 Ma (Mudelsee and Raymo, 2005), and immediately predating the well-studied Pliocene Research, Interpretation and Synoptic Mapping (PRISM) interval (Dowsett, 2007). We were drawn to revisit the original composite section because features surrounding the M2 glacial event seemed anomalous in comparison to other time-equivalent marine sections we have been investigating. We construct a more reliable composite section through a combination of tying high resolution measurements made at offset holes to a high-resolution downhole log acquired at Hole 846B, and we supplement that stratigraphic analysis with new stable isotopic and alkenone sea surface temperature (SST) estimates from hole 846B, which was not used in the original composite in the M2 interval. We propose a revised composite section spanning the interval equivalent to the early Gauss through Mammoth magnetic polarity zones (circa 3.2-3.6. Ma) and tie the ODP Site 846 records to ODP Site 850, which provides an indirect tie of stable isotopic and SST estimates at Site 846 to a high-quality magnetic polarity stratigraphy. Our results also yield insights into core recovery and coring distortion artifacts during hydraulic piston coring of calcareous-siliceous sediments of the equatorial Pacific.

2   Methods

1.1 Composite section generation

Assignments of gaps in core recovery and distortions induced by coring create challenges in accurately compositing sedimentary records from offset holes. The scientific part on board Leg 138 made excellent use of high-resolution measurements from the Gamma Ray Porosity

Evaluation scanner, a reflectance spectrophotometer, and magnetic susceptibility logging of cores (Hagelberg et al., 1995; Mix et al., 1995). Constructing a composite section proceeded by identifying tie points between holes on a core-by-core basis, splicing missing material at core
80   breaks by the section represented at an offset hole, and assuming that a linear offset applied between the drilling depth (mbsf) and the composite depth that resulted from splicing materials between holes. As compared to the original drilling depth, the composite section at Site 846 grew by about 15%, indicating that a significant amount of material was not recovered at any one hole during drilling.
85

Later sampling followed the logic of the initial splicing, hopping between holes to follow the composite section documented in the Initial Reports volume (Hagelberg et al., 1992, 1995). A more flexible and robust procedure for composite section generation was subsequently developed using dynamic programming to optimally align time series data (Lisiecki and Lisiecki,
90   2002, and Lisiecki and Herbert, 2007. This method allowed for assessing distortions in the coring process (e.g. stretching or squeezing of sedimentation relative to the undisturbed section) but it still required user guidance of key tie points and the more or less arbitrary assumption of which section of several replicates (e.g. holes B, C and D at Site 846) provided the least disturbed representation of sedimentation.
95

In this work we continue to use the Match program developed by Lisiecki and Lisiecki (2002), but take advantage of a high resolution downhole log of conductivity acquired at the time of drilling, which provides the best representation of a truly continuous and undistorted sedimentary column at Site 846. This opportunity was not recognized in the compositing of Lisiecki and
100   Herbert (2007), although it could have been apparent based on the work of Harris et al. (1995), who used a different hostile-environment lithodensity sonde (HLDS)
log that has lower spatial resolution than the Formation Microscanner (FMS) conductivity sensor log analyzed here. The FMS log (Hole 846B pass 2) acquired data at 0.25 cm resolution from ~80 mbsf (early Pleistocene) to the base of the section (see
105   http://brg.ldeo.columbia.edu/logdb/hole/?path=odp/leg138/846B/). Unlike many of the borehole logging measurements, the conductivity log preserves fine scale (centimetric) variations related to changes in lithology and sediment physical properties. The conductivity measurements essentially represent the inverse of porosity logging, as conductivity increases with conductive pore water volume and decreases as the volume of solids grows. The conductivity log is
110   therefore quite similar to variations in wet bulk density logged by the Gamma Ray Attenuation Porosity Evaluator (GRAPE) sensor in cores raised during drilling of Site 846 (Figure 1 reports highly significant correlations of detrended data FMS and GRAPE). As demonstrated by shipboard results, wet bulk density correlates positively with carbonate content and therefore positively with reflectance (r = 0.69 for datasets from Site 846).
115

The downhole log information includes conductivity measurements from three pad sensors. We tested different combinations of weighting the log data against reflectance and GRAPE time series measured on cores (mean, geometric mean, maximum/minimum of the 3 measurements) and found that choosing the minimum of the 3 sensor measurements at each depth interval gave
120   consistently the highest match to the core color reflectance and GRAPE data sets. We interpret this result to reflect the likelihood that high conductivity readings can result from poor pad contact with the borehole and/or washouts of sediment, and are likely to be outliers. We also

found that one interval of the borehole provided unreliable data from any of the sensors, most
likely due to a significant washout, and deleted data from this segment (138.37 to 138.19 meters
in log depth) in our alignment process. Three more short segments showed unusually low
conductivity and were likewise removed (146.6799-146.746, 150.3299-150.3705, and 150.4315-
150.4798 meters log depth). We used core photographs to remove GRAPE and reflectance
outliers at the top and base of cores based on visual evidence of core disturbance.

Mapping between offset holes and the downhole conductivity log was done to optimize the
alignment of GRAPE and reflectance data to the target. In addition, guided by the downhole log,
we optimized the alignment of each offset hole data to the other offset holes. Data sets were
normalized and detrended and we mapped ( ) reflectance and GRAPE bulk density to (-)
conductivity. While we relied on the reflectance and GRAPE information, wherever possible we
checked for consistency with stable isotopic (Shackleton et al., 1995b) and alkenone (Lawrence
et al., 2006) data sets as well. Tie points were inserted based on both reflectance and GRAPE
data, but the final composites were generated from the Match algorithm applied to the GRAPE
time series only, as this consistently showed better alignment to the log and smoother variations
in implied core distortion than the reflectance data. The better correlations to the borelog log via
GRAPE presumably reflects the benefit of consistent GRAPE calibration to density standards in
comparison to the reflectivity measurements and/or a closer match between GRAPE-estimated
wet bulk density and conductivity, in comparison to color reflectance.

Our goal in composite section generation was to achieve alignments between the depth series of
offset holes and the conductivity log robust at the scale of orbitally-related variations in
sedimentation and proxy variance. Given sedimentation rates in the interval of interest of 4-5
cm/kyr, this meant achieving satisfactory alignment at ~40 cm, or one half precessional
wavelength. In practice, we found that approximately 20 tie points served to achieve this level of
match. The Match algorithm includes a number of tradeoffs in the alignment procedure.
Essentially, it determines the optimal alignment of segments of data at integer ratios, with a 1:1
alignment indicating no distortion of one record relative to the other. In addition to default
choices supplied by the Match software (http://lorraine-lisiecki.com/match.html) we ran an
experiment where we increased the number of integer choices in the vicinity of the 1:1 match in
order to suppress smalls-scale jumps in relative accumulation in order to see larger patterns
between offset holes (the point penalty score for correlations to the log can be improved by about
15% by letting the accumulation rate change more freely in the Match algorithm than we do for
the "smooth" mapping). To enhance smoothness, we assigned a relatively high penalty function
to the speed parameter but very little penalty to the speed change parameter- this allowed for fine
scale adjustment of relative accumulation rates while minimizing large and abrupt changes in the
mapping functions. We also iteratively adjusted the gaps assigned between cores from the
nominal gaps determined by the shipboard splices, so that the matching procedure yielded a
smooth downhole mapping without artificial jumps at core breaks (Figures 2 and 3.

Ultimately, we determined that choices such as the number of intervals and penalty parameters
had very little effect on the final mapping (e.g. variations in parameters by a factor of 2 produced
negligible changes in mapping). Final Match parameter choices are presented in Table I.
Figure 2 portrays the final alignment of individual GRAPE time series to the downhole
conductivity log at Site 846. At Site 850, we produced a composite section from simultaneous

alignment of GRAPE, reflectance, and magnetic susceptibility measurements at holes 850A and
850B. This composite has no downhole log reference section; however, the composite allows us
to very accurately map discrete measurements between holes A and B of alkenone unsaturation
and stable isotopes produced as part of the present work. Composite reflectance, GRAPE and
magnetic susceptibility (for Site 850) sections are included as Supplementary Tables 1-13.

1.2 Stable isotopic data

Because our initial investigation suggested an ambiguity in the composite section based on
splices of holes 846D (which provides the majority of the backbone to the shipboard composite
section) to 846C in the interval 95 to 181 meters composite depth (mcd) as defined by the
shipboard scientific party (splice of 846D core 13 to 846 C core 13 and then to 846D core 14),
we analyzed 227 new samples from hole 846B, cores 12, 13, and 14, of which 211 yielded
enough benthic foraminifera for isotope analysis at the Brown University stable isotope facility.
Samples were freeze-dried, soaked in water for 24 hours to disaggregate, and wet sieved using a
150 μm mesh. Samples were then dried at 40 °C and split into a faunal and isotope fractions.
Isotope fraction vials were dry sieved, benthic foraminifera were picked from 150-355 μm,
cleaned with 70 μl ethanol, sonified for 30 seconds, ethanol was drawn off with a pipette, and
specimens were dried overnight at room temperature. In some cases, it was necessary to expand
the size fraction to 150-355 μm to provide enough carbonate for replicate measurements. Isotope
ratios were quantified at with a Finnigan MAT 252 with Carbonate Kiel III autosampler, where
the individual sample is reacted with 70 °C H_3PO_4.   170 of the 211 intervals were analyzed at
least in duplicate, and in a number of cases we were able to acquire triplicate or quadruplicate
replication. We analyzed both *Cibicidoides wuellerstorfi* and *Uvigerina peregrina* (95 paired
samples) and determined an average offset of 0.643 ± 0.011 °/$_{oo}$ (standard error of the mean) for
$\delta^{18}O$ (*Uvigerina* heavier) and   0.973 °/$_{oo}$ for $\delta^{13}C$ (*Cibicidoides* heavier, ± 0.018 standard error
of the mean). At Site 846, we supplemented analyses with a handful (15) of measurements on
Cibicidoides mundulus where *C. wuellerstorfi* and/or *U. peregrina* were not abundant enough to
provide a good signal for mass spectrometry. In accordance with standard practice (Duplessy et
al., 1984; Shackleton & Opdyke, 1973), *Cibicidoides* $\delta^{18}O$ values were adjusted to *Uvigerina*
values; similarly, *Uvigerina* carbon isotope values were adjusted to *Cibicidoides*. *C. mundulus*
isotopic values were taken as equivalent to *C. wuellerstorfi*. Wherever replicate analyses were
possible, we report results as the average.

At Site 850, we obtained 273 samples from Holes A (core 7) and B (cores 6 and 7) where benthic
foraminifera were sufficient for isotope analysis (we had smaller sample volumes, so the data set
is less continuous than for Site 846). Replication is also less extensive (155 of 273 samples) and
the proportion of *C. mundulus* used was higher (63 samples). Isotopic adjustments by species
were handled identically to those at Site 846.

When we compared stable isotopic data acquired at Brown with values reported by Shackleton et
al. (1995b) over the equivalent interval at holes 846D and C it was evident that there was an
isotope offset of 0.17 in $\delta^{18}O$ (Brown heavier). Variance was essentially identical; therefore, we
adjusted the Brown values to align with the much longer Shackleton et al. (1995b) record by
adjusting the Brown $\delta^{18}O$ values by the average difference. It is not clear that the choosing the

215   Shackleton values is preferable on analytical grounds, but our choice allows the user to incorporate our new splice without having to adjust previously published values determined by the Shackleton et al. (1995b) study. We found no statistically significant offset between the carbon isotope values determined at Brown and the values in Shackleton et al. (1995b). The oxygen and carbon species-specific isotopic offsets we report are identical with (δ^{18}O) or

220   very similar to (δ^{13}C) the offsets used by Shackleton et al. (1995b).

1.3 Alkenone unsaturation estimates

225   Alkenone paleothermometry relies on the temperature dependence of the degree of unsaturation (number of double bonds) observed in the suite of organic compounds ($C_{37:3}$ and $C_{37:2}$ alkenones) synthesized by marine surface-dwelling haptophyte algae (Marlowe et al., 1984; Prahl and Wakeham, 1987). Alkenone extraction followed freeze-drying ~1 g of homogenized dry sediment, using 100% Dichloromethane (DCM) and a Dionex 200 Accelerated Solvent Extractor

230   (ASE. Prior to quantification, extracts were evaporated with nitrogen and reconstituted with 200 µL of toluene spiked with n-hexatriacontane (C_{36}) and n-heptatriacontane (C_{37}) standards. Alkenone parameters were determined using an Agilent Technologies 6890 gas chromatograph–flame ionization detector (GC-FID), with Agilent Technologies DB-1 column (60 m, 0.32 mm diameter and 0.10 mm film thickness. Procedure entailed a 1µl injection, initial temperature 90

235   °C, increased to 255 °C with 40 °C/minute rate, increased by 1 °C/minute to 300 °C, increased by 10 °C/minute to 320 °C, and an isothermal hold at 320 °C for 11 minutes. All GC analyses simultaneously provide the information to determine the $U^{K'}_{37}$ unsaturation values and an estimate of the total amount of C_{37} ketones by summation of the areas of the $C_{37:2}$ and $C_{37:3}$ alkenones. Long-term laboratory analytical error, estimated from replicate extractions and gas

240   chromatographic analyses of a composite sediment standard is equivalent in temperature to ±0.1 °C.

We analyzed a total of 249 samples from hole 846B and 427 from holes 850A and 850B. All samples yielded adequate alkenone concentrations for unsaturation estimates. The mean $U^{k'}_{37}$

245   value for the interval of interest from hole 846B of 0.896 compares very well to the average reported by Lawrence et al. (2006) from equivalent interval of hole 846D of 0.902, although small differences in orbital-scale peak amplitudes are observed that probably reflect small variations in gas chromatographic performance over time. For consistency to the longer Lawrence et al. record, we adjusted new Uk'37 values by .006. To convert to estimated sea

250   surface temperature (SST) we used the global core top calibration of Muller et al. (1998).

2   Results

3.1 Lessons on coring distortion

255

The Lisiecki and Herbert (2007) study of hydraulic piston coring relied on offset holes alone to assess distortion related to porosity rebound and coring-induced disturbance. This meant that distortion could be assessed from one hole *relative* to another, but without a definitive undistorted reference (with the exception of reported drilling depth at the top and bottom of each

260   core). In the present case, we can assess distortions using the Match alignment of composite

sections to the presumably undistorted conductivity borehole log. Several conclusions stand out. First, there are very few instances of coring compression indicated by the Match algorithm (compression would register as a relative accumulation rate < 1) (Figure 3). Second, we can only document one instance of coring repetition, a segment of ~40 cm at the top of 846B core 16,

265 consistent with the original composite section proposed by the shipboard party.

Lisiecki and Herbert (2007) found strong correlations of extension for Leg 138 sites with %CaCO$_3$, and GRAPE density for the upper 50m, but decreasing correlation at depth. Our mapping of each offset hole to the downhole log shows a relationship of coring distortion

270 between the inverse of log conductivity, composite GRAPE density, and composite reflectance (not shown) over the study interval using the smoother fit option (e.g. more Match speed choices close to 1:1 between cores and the downhole log) (Figure 3). Most of the distortions correlate between offset holes (Figure 3), demonstrating the largely predictable coring expansion with lithological variations. In the case of these siliceous sediments, the coring distortion may also be

275 related to lithology as well as physical properties, as zones with lower density (higher porosity) generally have high biogenic silica contents and may behave differently from carbonate-dominated lithologies during coring. While the distortion appears systematic, it somewhat counter-intuitively indicates expansion of the lower conductivity (higher carbonate/lower porosity) beds relative to lower carbonate beds when examined in detail, although the

280 relationship is not statistically significant (Figure 4) and may depend on unresolved factors such as differences in the proportion of biogenic silica to detrital content in the non-carbonate fraction, or to the *contrast* of physical properties with depth. Evaluating distortion as a function of position within each core fails to reveal systematic distortion as a function of the HPC barrel penetration (Figure 5). It therefore seems as if there is little differential distortion during the

285 stroke of the HPC that cannot be explained by the behavior of contrasting lithologies penetrated.

We also found that our new composites of reflectance and GRAPE density (see Tables S2-S7) compare much more favorably to the downhole log data than the prior Lisiecki and Herbert (2007) composite. We attribute the better match both to the use of a continuous log reference

290 and to the additional splicing constraints gained from consulting stable isotopic and alkenone data. This observation highlights the importance of incorporating all available stratigraphic data to avoid mistakes in tying potentially ambiguous sections between offset holes so as to generate the most reliable composite section.

295

3.2 Revision of the Mammoth-Gauss/Gilbert equivalent section

To generate a revised composite, we used the downhole conductivity log as our reference. The Match algorithm allows a continuous mapping of reflectance and GRAPE data at offset

300 Holes 846B, 846C, and 846D with log depth as the common depth scale (Tables 2-7). Data obtained from any of the offset holes can be correlated to this reference depth with an uncertainty on the order of 5 cm (resolution of Match alignment). The original shipboard splice links holes 846D (the primary hole used by Shackleton et al., 1995b, and followed by Lawrence et al. 2006) and 846C. As Figure 6 demonstrates, recovery at hole 846C entirely omits the M2 interval. We

305 turn to hole 846B, which contains the best representation of both the M2 interval and the subsequent interglacial recovery, to tie its record to hole 846D. The original composite using

hole 846C does nearly completely tie the gap between cores 12 and 13 of hole 846B, but is extremely stretched for the last ~2 meters by coring distortion (Figure 6). The tie lines indicated in Figure 6 include important constraints from the GRAPE log and from our new discrete $\delta^{18}O$

310 and alkenone measurements (not shown) in addition to the reflectance data displayed. Table 8 provides the new composite section as a sequence of discrete segments from the different offset holes. Log depth again provides the new composite depth.

The original $\delta^{18}O$ section published by Shackleton et al. (1995b) in the vicinity of the M2 glacial

315 event seems unusual in having 2 distinctly separated enriched features (Figure 7) - an anomaly that showed clearly in the original LR04 isotope stack (Figure 9 of Lisiecki and Raymo, 2005), but that nevertheless guided the final product of that stack. Carbon isotopes (not shown) also show an anomalous depletion in the same interval. Turning to a high-resolution SST record previously generated at Site 846 (Lawrence et al., 2006), it too seems anomalous, in that a strong

320 cooling is very short lived and does not follow the reflectance, GRAPE, and stable isotopic trends well in this particular interval (Figure 9). As documented below, we are convinced that an error of unknown origin at Site 846 (erroneously labeled samples? Inverted core section?) has confused the stratigraphy surrounding the M2 event.

325 Both the stable isotopic and alkenone data previously generated at hole 846D deviate in an anomalous manner relative to reflectance and GRAPE variations in the M2 interval (Figures 7 & 8). In general, the isotopic and alkenone values align well with variations in reflectance, log conductivity and also GRAPE bulk density at Site 846; this is the only interval we have observed with such significant deviations between proxies. In contrast, if we exclude the problematic

330 intervals identified in Figure 9 (specifically, stable isotope data from 846D core 13, section 1, and alkenone data from 846D core 13, section 2), the new composite that integrates newly generated stable isotopic and alkenone data from hole 846B follows reflectance and log data closely through the interval containing the M2 glacial event (Figure 9). It is therefore apparent that, for unknown reasons, both previously published isotopic and alkenone data that followed

335 the original splice in the M2 interval are not reliable. We attempted several simple fixes, such as assuming that stable isotope data from hole 846D, core 13, section 1, were reversed in depth by a sampling error, but the data still would not align well with the new isotope section from hole 846B, or with the reflectance and GRAPE data generated on the same section at 846D. We conclude that stable isotopic data from 846D, core 13, section 1, and alkenone data from 846D,

340 core 13, section 2 must be discarded as erroneous. In addition, the original splice from 846D, core 12 to 846C, core 12 is problematic because of what appears to be extensive coring extension at the base of core 12 at Hole 846C (Figure 6).

We can confirm the reliability of the new isotopic and SST composites at Site 846 (see Tables S9

345 and S10) by comparing them to newly generated records at Site 850 (Figure 10; Table S11). The equivalent interval at Site 850 spans only one core break, minimizing possible uncertainties in creating a continuous composite section there. Unfortunately, the Pliocene section at Site 850 is too shallow to have had borehole logging, so we can only create a composite depth section based on coring (Tables S12-14). Nevertheless, isotopic and reconstructed SST patterns can be

350 matched very precisely (sample tie lines indicated in Figure 10) between Sites 846 and 850, once coring and/or sedimentation rate distortions are considered. These ties also allow us to indirectly

transfer the high-quality magnetic polarity stratigraphy obtained at Site 850 to its equivalent positions at Site 846 (Figure 10).

4 Conclusions

355

In our new composite, we align data from offset holes to the borehole conductivity log to obtain the least distorted representation of the mid to late Pliocene interval, focusing especially on the stratigraphy around the M2 interval. Careful analysis of the original composite section produced

360 at Site 846 shows errors of unknown origin in the critical interval surrounding the M2 glacial event. These errors influenced the original LR04 isotopic stack and the composite tropical ocean temperature stack of Herbert et al. (2010), and persist in the recent Ahn et al. (2017) revision to LR04, although to a lesser degree as more sites have been incorporated into the new isotopic stack. In contrast to the earlier data sets from Site 846, the M2 glaciation now stands out as a

365 long sawtooth feature of enriched $\delta^{18}O$ and cold SST values, rather than as 2 events separated by a significant deglaciation/warming. The anomalously enriched interval of the $\delta^{18}O$ record preceding the M2 glaciation identified as MG4 in LR04 (see Figure 9 of Lisiecki and Raymo, 2005) seems to be a 1-point outlier when new isotopic information from Hole 846B is spliced into the revised composite (Fig 8). We suggest that the new splice and composite section shown

370 in Figure 9 replace the previously published alkenone and stable isotope sections of Lawrence et al. (2006) and Shackleton et al. (1995b) and that this revised section (see Supplementary Tables S8 and S9) be incorporated in future stable isotope and temperature stacks. Given the expanded sedimentation rate and dense sampling resolution of stable isotopic and alkenone data at Site 846, this new composite provides one of the best representations of late Pliocene

375 paleoceanographic variability.

Code/Data Availability

Composite sections of non-destructive measurements (reflectance, GRAPE wet bulk density, magnetic susceptibility, borehole conductivity log from Site 846) at Sites 846 and 850 are
380 available, with primary (hole, core, section, and centimeter depth) as well as derived (composite depth) information included. New stable isotopic and alkenone determinations at Sites 846 and 850 with primary and derived (composite depth) information are also reported. All data are available as tab-delimited text files archived on the website Pangaea.

385 ## Author Contribution

T. Herbert produced composite sections using the Match algorithm and wrote the bulk of the manuscript. All authors contributed to manuscript revision. R. Caballero-Gill produced alkenone SST estimates at Sites 846 and 850 and helped in the construction of composite sections. J.B. Novak picked foraminiferal samples for stable isotopic analysis and supervised
390 running samples at the Brown Stable Isotope Facility.

Competing interests

The authors declare that they have no competing interests associated with this manuscript.

395 ## Acknowledgements

N.S.F. grants OCE-1459280 and PIRE-1545859 supported Herbert and Caballero-Gill during this project; stable isotopic analyses and alkenone analyses were also supported by H.J. Dowsett of the U.S. Geological Survey.   The authors gratefully acknowledge the curators of the Integrated Ocean Drilling Program for providing samples from ODP Sites 846 and 850.
400

References cited

405

Ahn, S., Khider, D., Lisiecki, L. E., and Lawrence, C. E.: A probabilistic Pliocene–Pleistocene stack of benthic δ18O using a profile hidden Markov model, Dynamics and Statistics Climate Sys., 2, https://doi.org/10.1093/climsys/dzx002, 2017.

410 Dowsett, H.: The PRISM palaeoclimate reconstruction and Pliocene sea-surface temperature in Deep-time perspectives on climate change: Marrying the signal from computer models and biological proxies, edited by: Williams, M., Haywood, A.M., Gregory, F.J., and Schmidt, D.N., London, The Geological Society, Micropaleontological Society Special Publications, p. 459-480, 2007.

415

Duplessy,J.C, Shackleton, NJ., Matthews,R.K., Prell,W. Ruddiman, W.F., Caralp,M. and Hendy, CH., 1984. ^{13}C record of benthic foraminifera in the last interglacial ocean: implications for the carbon cycle and the global deep water circulation. Quat. Res., 21:225-243.

420 Hagelberg, T.K., Pisias, N.G., Shackleton, N.J., Mix, A.C., and Harris, S.E.: Refinement of a high-resolution, continuous sedimentary section for studying equatorial Pacific Ocean paleoceanography Leg 138. In: Pisias, N.G., Mayer, L.A., Janecek, T.R., Palmer-Julson, A., and van Andel, T.H. (Eds.), Proceedings of the Ocean Drilling Program, Scientific Results (vol. 138, p. 31-46), 1995.

425

Harris, S. E., Shackleton, N.J., Hagelberg, T.K., Pisias, N.G. and Mix, A.C.: Sediment depths determined by comparison of grape and logging density data during Leg 138, Proceedings of the Ocean Drilling Program, Scientific Results, Vol. 138, edited by: Pisias, N.G., Mayer, L.A., Janecek, T.R., Palmer-Julson, A., and van Andel, T.H., College Station, TX (Ocean Drilling
430 Program), 47-57, 1995.

Herbert, T.D., Cleaveland Peterson, L., Lawrence, K.T., and Liu, Z.: Tropical ocean temperature over the past 3.5 million years, Science, 328, 1530-1534, 2010.

435 Lawrence, K.T., Liu, Z., and Herbert, T.D.: Evolution of the eastern tropical Pacific through Plio-Pleistocene glaciation, Science, 312, 79-83, 2006.

Lisiecki, L.E. and Herbert, T.D.: Automated composite depth scale construction and estimates of sediment core extension, Paleoceanography 22, DOI: 10.1029/2004PA001071, 2007.
440

Lisiecki, L.E. and Lisiecki, P.A.: Application of dynamic programming to the correlation of paleoclimate records, Paleoceanography, 17, https://doi.org/10.1029/2001PA000733, 2002.

Lisiecki, L.E. and Raymo, M.E.: A Pliocene-Pleistocene stack of 57 globally distributed benthic δ^{18}O records, Paleoceanography, 20, doi:10.1029/2004PA001071, 2005.

445   Marlowe, I., Green, J., Neal, A., Brassell, S., Eglinton, G., Course, P.: Long chain (n-C37–C39) alkenones in the Prymnesiophyceae. Distribution of alkenones and other lipids and their taxonomic significance, British Phycol. J., 19, 203-216, 1984.

Mix, A. C., Harris, S.E., and Janecek, T.R.: Estimating lithology from nonintrusive reflectance spectra: Leg 138, Proceedings of the Ocean Drilling Program, Scientific Results, vol. 138, edited
450   by: Pisias, N.G., Mayer, L.A., Janecek, T.R., Palmer-Julson, A., and van Andel, T.H., College Station, TX (Ocean Drilling Program), 413-428, 1995.

Mudelsee, M. and Raymo, M.E.: Slow dynamics of the Northern Hemisphere glaciation, Paleoceanography 20(4) https://doi.org/10.1029/2005PA001153, 2005.
455
Müller, P. J., Kirst, G., Ruhland, G., von Storch, I., and Rosell-Melé, A.: Calibration of the alkenone paleotemperature index U K′ based on core-tops from the eastern South Atlantic and the global ocean (60° N-60° S), Geochim. Cosmochim.Acta, 62, 1757-1772, 1998.

460   Prahl, F. G. and Wakeham, S.G.: Calibration of unsaturation patterns in long-chain ketone compositions for paleotemperature assessment, Nature, 330, 367-369, 1987.

Shackleton, N., Crowhurst, S., Hagelberg, T., Pisias, N., and Schneider, D.: A new Late Neogene time scale: application to Leg 138 sites. Proceedings of the Ocean Drilling Program, Scientific
465   Results, Vol. 138, edited by: Pisias, N.G., Mayer, L.A., Janecek, T.R., Palmer-Julson, A., and van Andel, T.H., College Station, TX (Ocean Drilling Program), 73-101, 1995a.

Shackleton, N., Hall, M.A., and Pate, D.: Pliocene stable isotope stratigraphy of Site 846, Proceedings of the Ocean Drilling Program, Scientific Results, Vol. 138, edited by: Pisias, N.G.,
470   Mayer, L.A., Janecek, T.R., Palmer-Julson, A., and van Andel, T.H., College Station, TX (Ocean Drilling Program), 337-355, 1995b.

Shackleton, N. J., & Opdyke, N. D. (1973). Oxygen isotope and palaeomagnetic stratigraphy of Equatorial Pacific core V28-238: Oxygen isotope temperatures and ice volumes on a 10^5 year
475   and 10^6 year scale, *Quaternary Research*, *3*, 39–55.

Shipboard Scientific Party: Site 846. In: Mayer, L., Pisias, N., Janecek, T. (Eds.), Initial Reports Ocean Drill. Progr., 138, 265- 333, 1992.

480   Table 1: values used with Match algorithm to generate "smooth" mappings of offset holes for new composite sections and for mapping to the borehole conductivity log. The default mapping for the "high resolution" mapping used speeds of 1:3, 2:5,1:2, 3:5, 2:3, 3:4, 4:5, 1:1, 5:4, 4:3,3:2, 5:3, 2:1, 5:2, and 3:1

485

Match parameter	
numintervals	2000 composites, 4000 to borehole log
nomatch penalty	40
speed penalty	45
target speed	1:01
tie penalty	60
gap penalty	40
speeds	10:7 4:3 9:7 5:4 6:5 7:6 8:7 9:8 10:9 11:10 13:12 21:20 31:30 1:1
	30:31 20:21 12:13 10:11 9:10 8:9 7:8 6:7 5:6 4:5 3:4 7:10

Supplementary Tables (archived on website Pangaea https://www.pangaea.de)

505

Figure 1. Locations of ODP Sites 846 and 850 (ODP Leg 138).
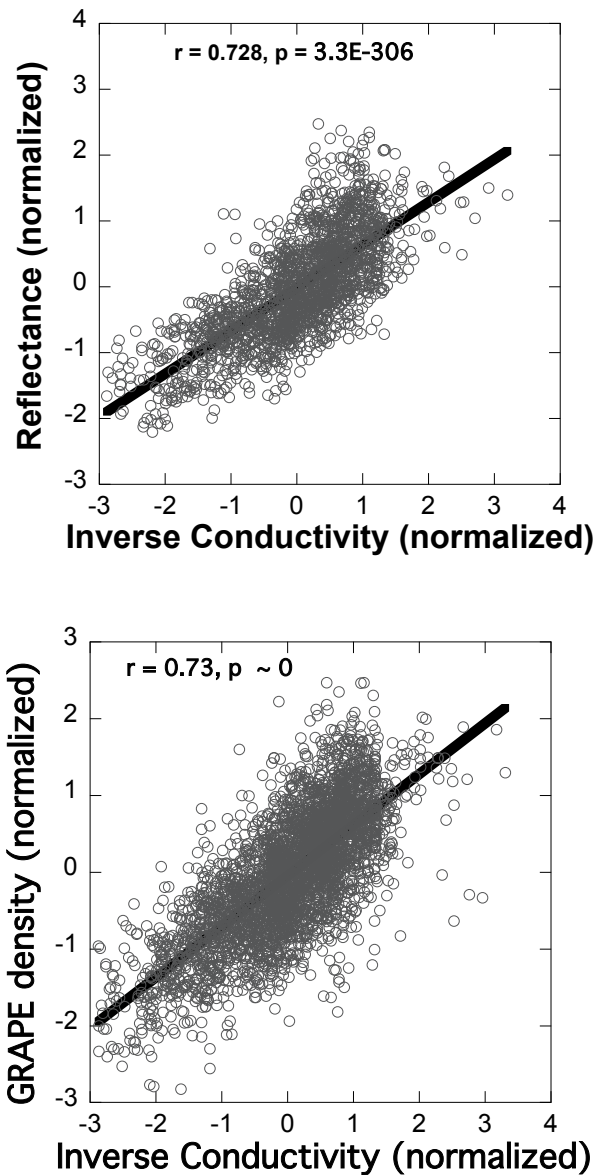
Figure 2. Correlations of the inverse of borehole log conductivity (detrended and normalized) to GRAPE density (detrended and normalized) and to color reflectance (channel 1, detrended and normalized) over the depth interval 85-170 mbsf (95-181 mcd), hole 846B. Note that the inverse of conductivity is plotted. Both correlations (N = 1853, 3388) are highly significant. Correlations of the same variables from holes 846C and 846D were very similar
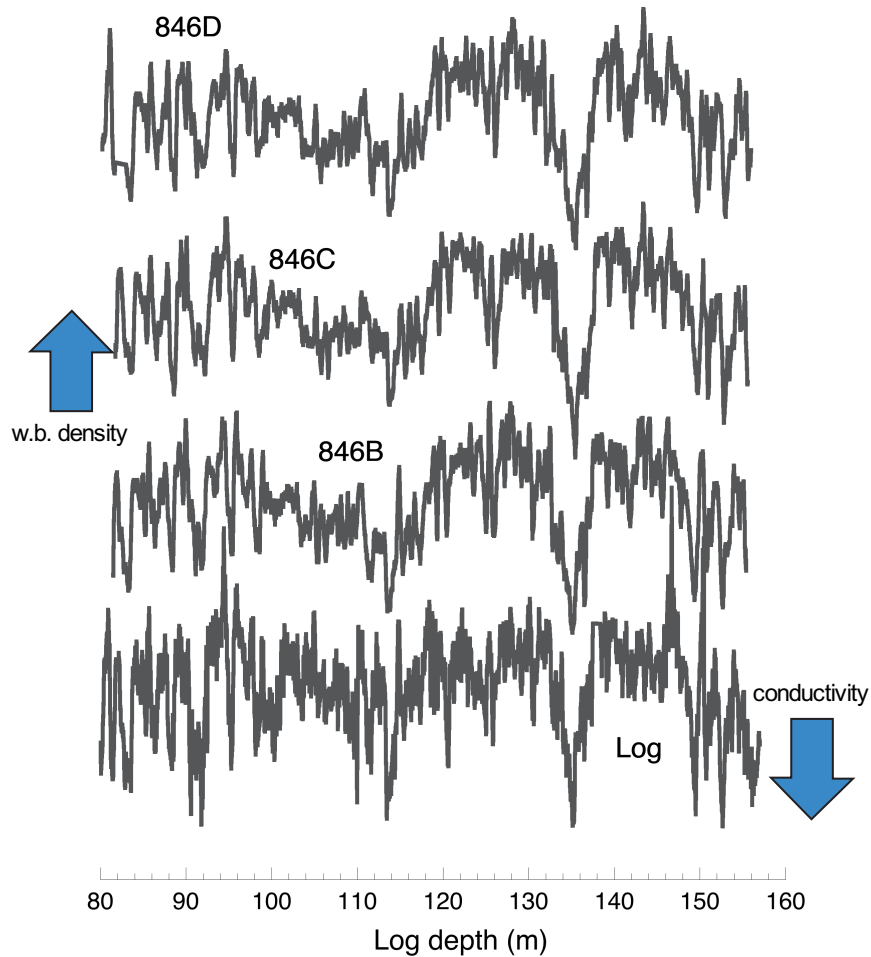
Figure 3. Composite sections of GRAPE density generated using the Match algorithm for holes 846B, C, and D, on a new composite depth section, compared to the inverse conductivity log depth. All data sets were detrended and normalized for this comparison. Coring gaps at each hole have been filled in from offset holes to make continuous splices.
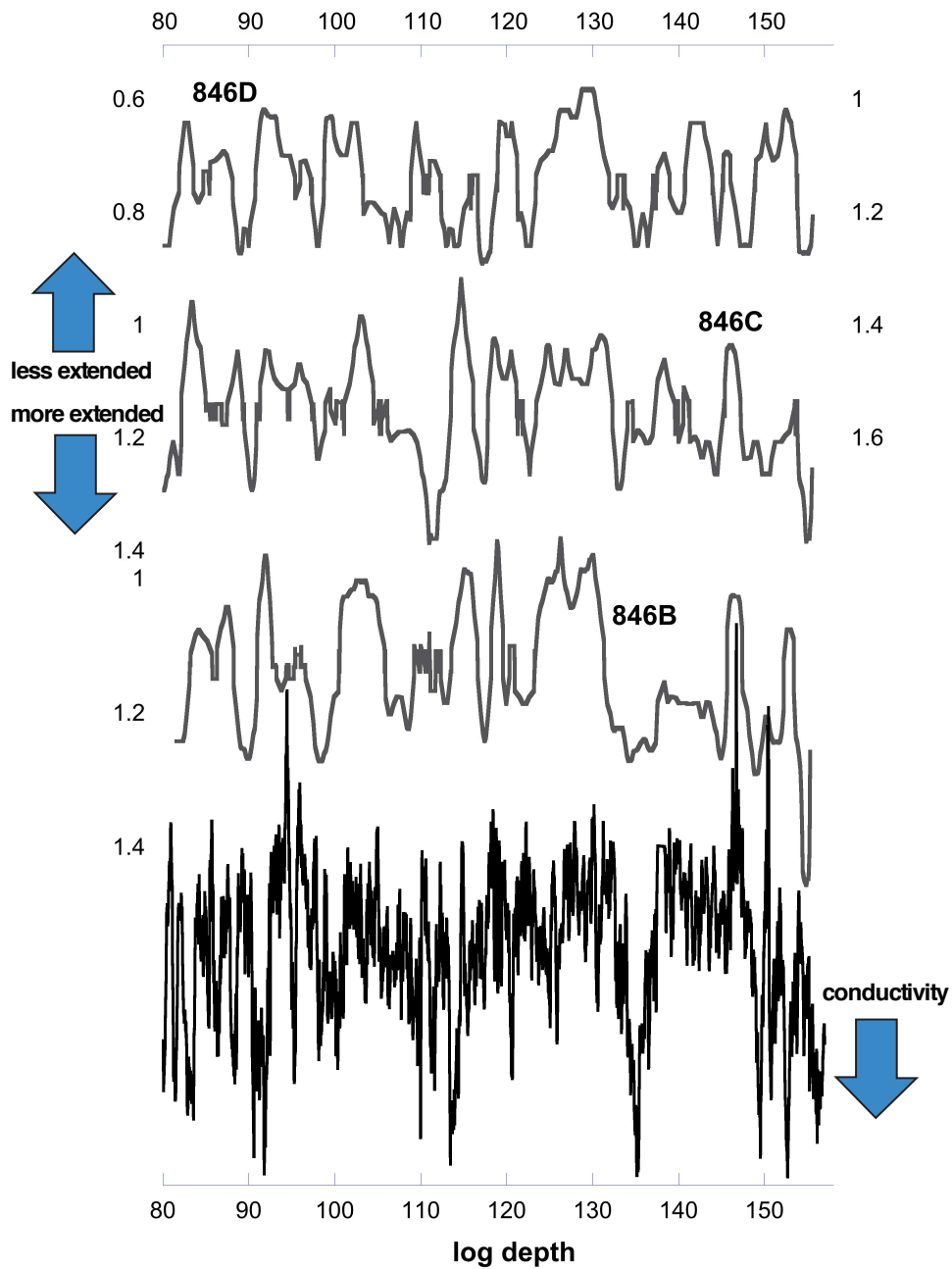
Figure 4. Coring distortion inferred from Match alignment of GRAPE composite sections to the borehole conductivity log (log has been inverted, detrended, and normalized) generated using the "smooth" Match parameters emphasizing a 1:1 depth mapping of core data to the downhole log. Values >1 indicates stretching of the cored section relative to the borehole log, which we assume represents the best representation of the in situ stratigraphy. Note that the scale for coring distortion has been inverted so that higher expansion (stretching) is in the downward direction.

510
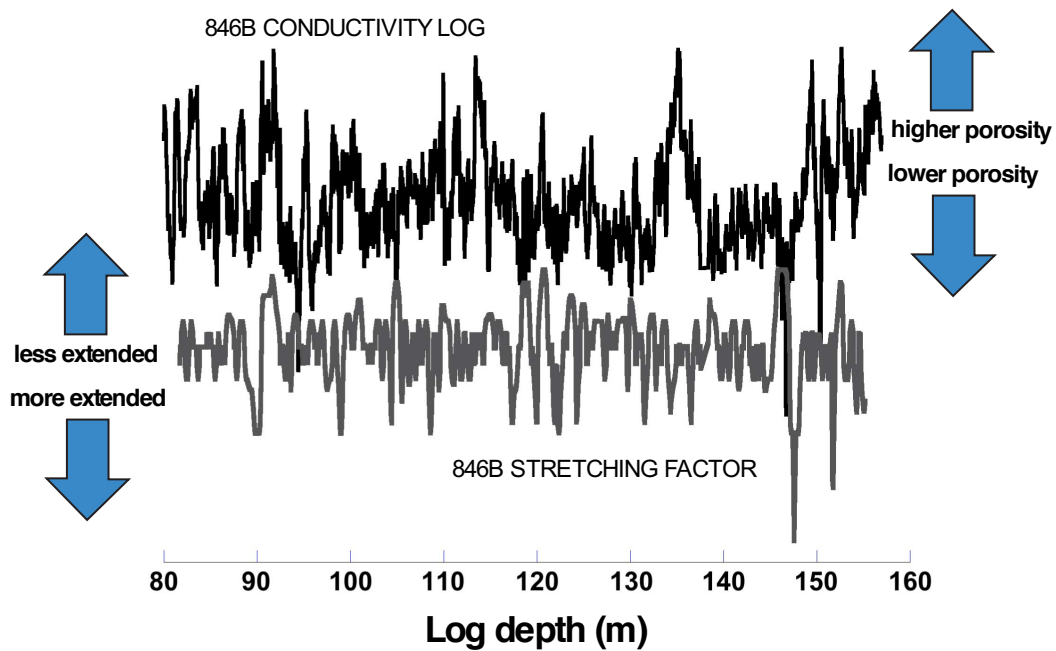
Figure 5. Coring distortion inferred from Match alignment of the hole 846B GRAPE composite section to the borehole conductivity log (conductivity data detrended and normalized) generated using the "high resolution" Match parameters emphasizing the closest possible mapping of core data to the downhole log. Note that core stretching generally moves positively with lower conductivity/porosity (higher carbonate content).
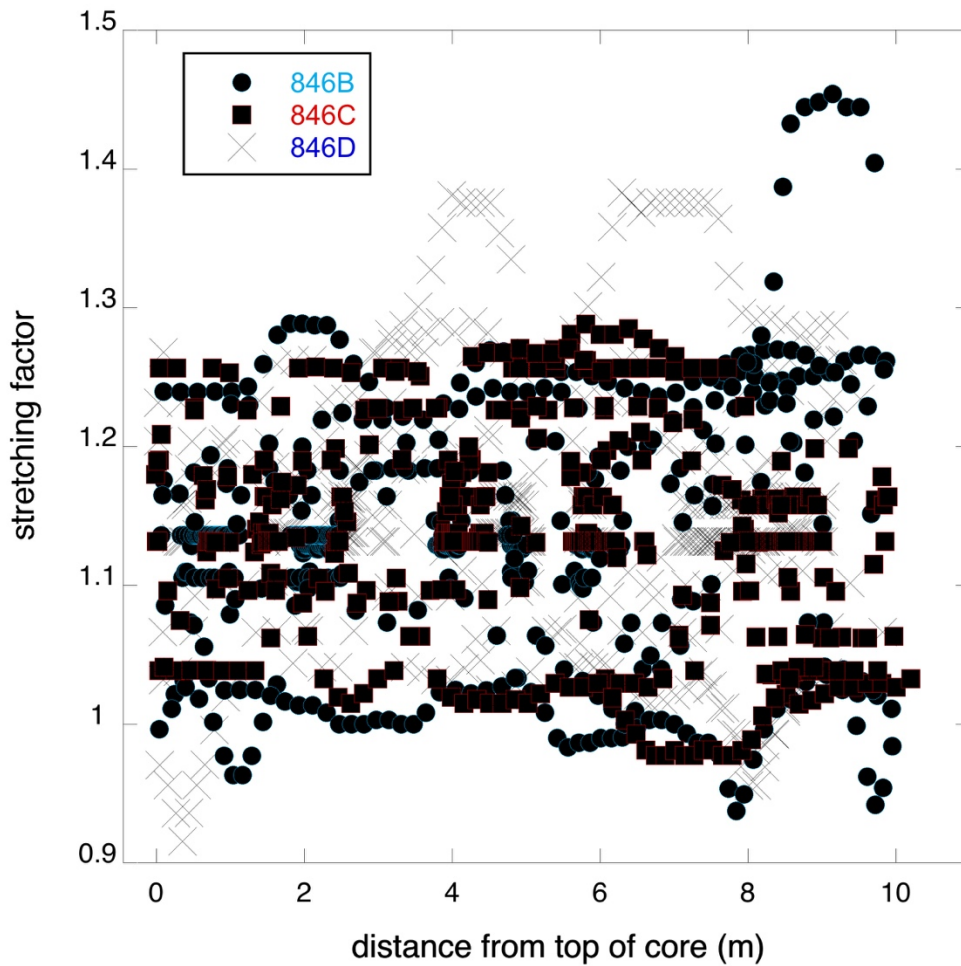
Figure 6. Inferred coring distortion based on Match alignment of GRAPE composite sections to the borehole conductivity log as a function of depth in each ~9.5 m core. Note that there is no evidence for a systematic pattern of stretching/squeezing as a function of penetration depth.
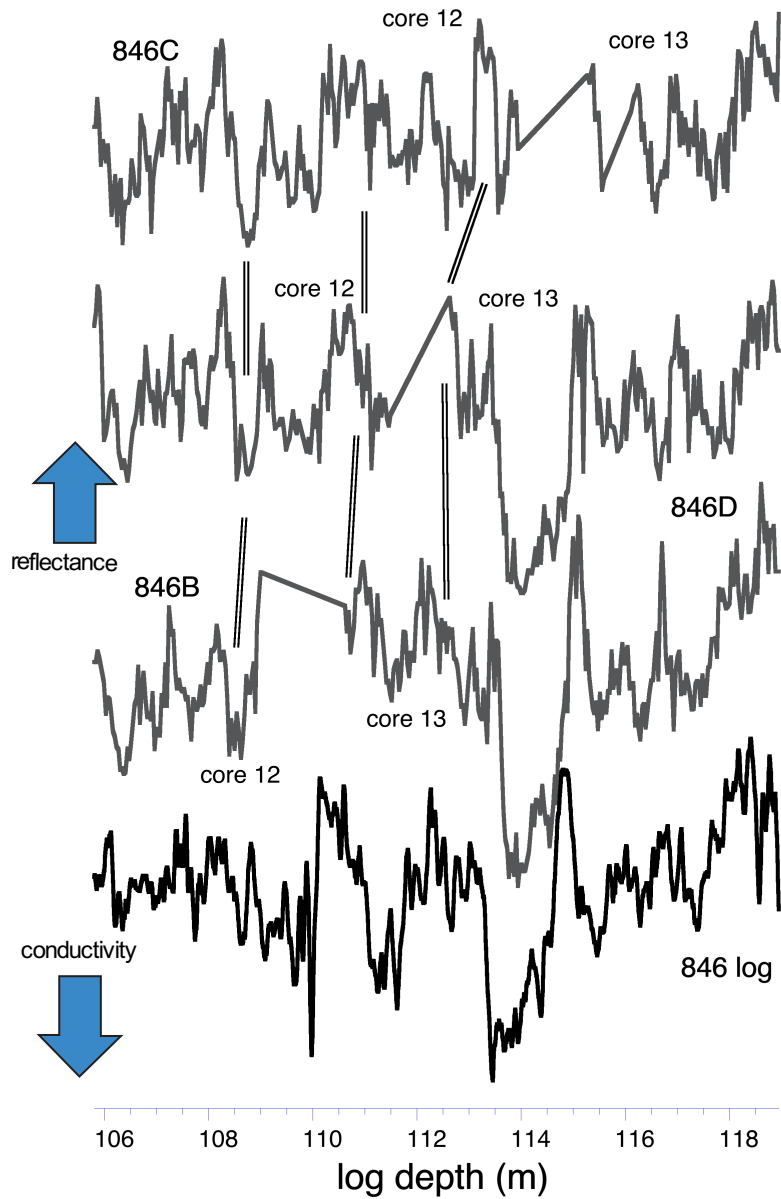
Figure 7. Detail of reflectance-based correlations (original mcd 122.6-137.8) of offset holes 846B, 846C, and 846D correlated to the common depth scale of the borehole log (log depth 106-119 m). Signals were detrended and normalized; higher reflectance and lower conductivity plot upward. Note the problematic tie of the base of Hole 846C, core 12 to the top of Hole 846D, core 13 (shipboard splice). In contrast, Hole 846B has a sequence that correlates easily to the borehole log and can be reliably spliced to the base of Hole 846D, core 12.
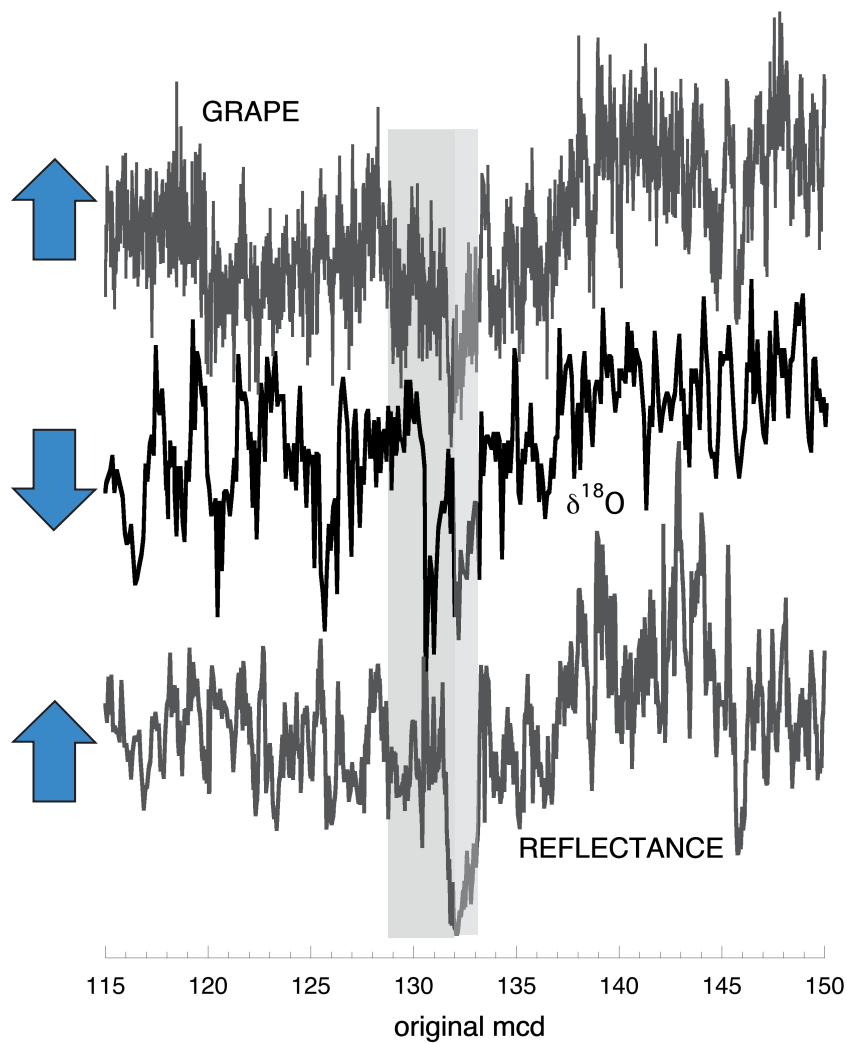
Figure 8. Comparison of $\delta^{18}O$ series of Shackleton et al. (1995b) on original composite depth (Shipboard Scientific Party, 1992) in comparison to reflectance and GRAPE data (original shipboard composite). Note the anomalous interval encompassing the M2 glacial event, indicated by gray shading where the isotopically enriched values depart from their correlation to reflectance and GRAPE values.
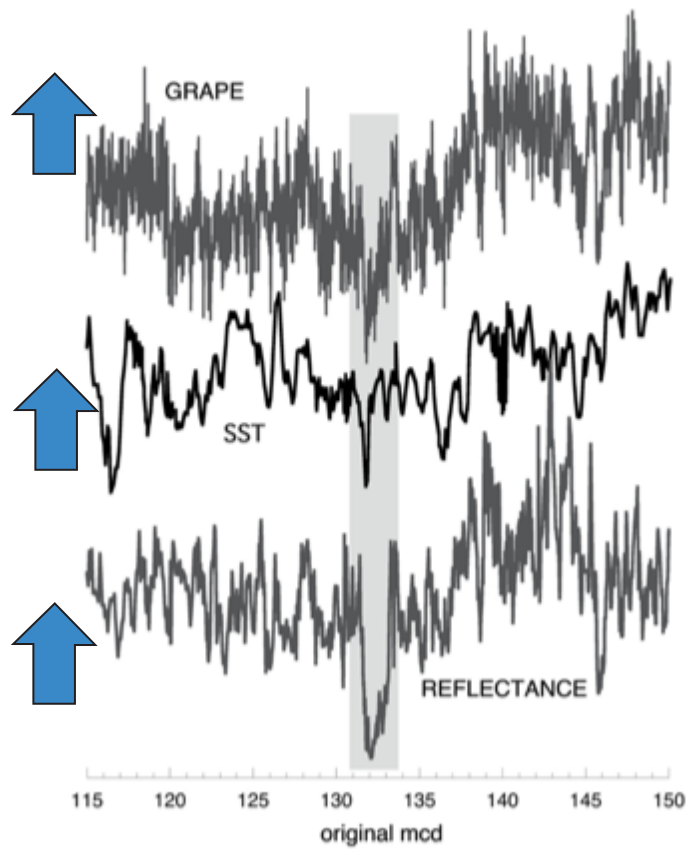
Figure 9. Comparison of alkenone-based SST series of Lawrence et al. (2006) on original composite depth in comparison to detrended and normalized reflectance and GRAPE data. Note the anomalous interval indicated by gray shading where the warm SST values depart from reflectance and GRAPE values.
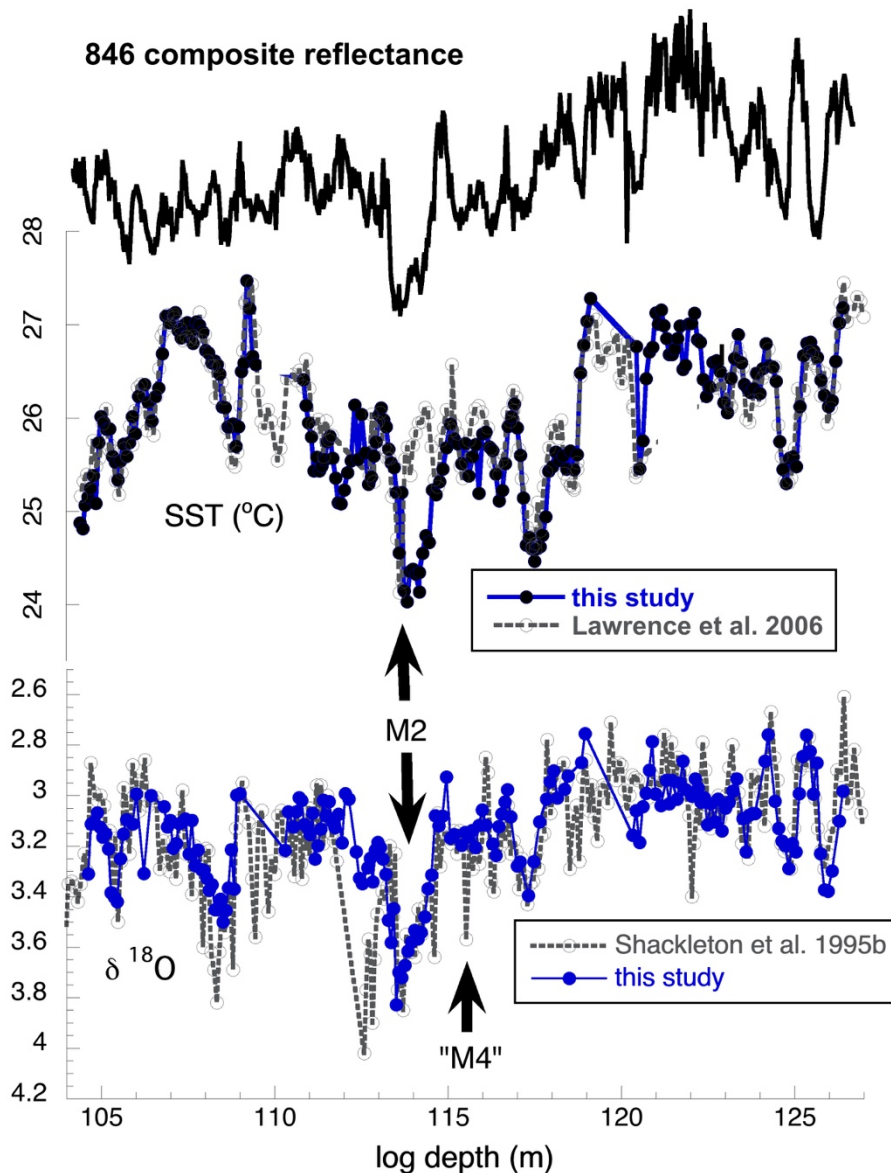
Figure 10. Revised alkenone and δ¹⁸O time series based on new data from hole 846B, aligned with prior data from Shackleton et al. (1995b) and Lawrence et al. (2006), excluding the problematic intervals around the M2 glaciation (see text. The composite section has been mapped to the borehole log depth. Previously published isotopic and alkenone data in the problematic M2 interval are shown as dashed lines. Revised composite time series now align well, and the interval containing the M2 glacial event presents as a sawtooth isotopic enrichment and cooling.
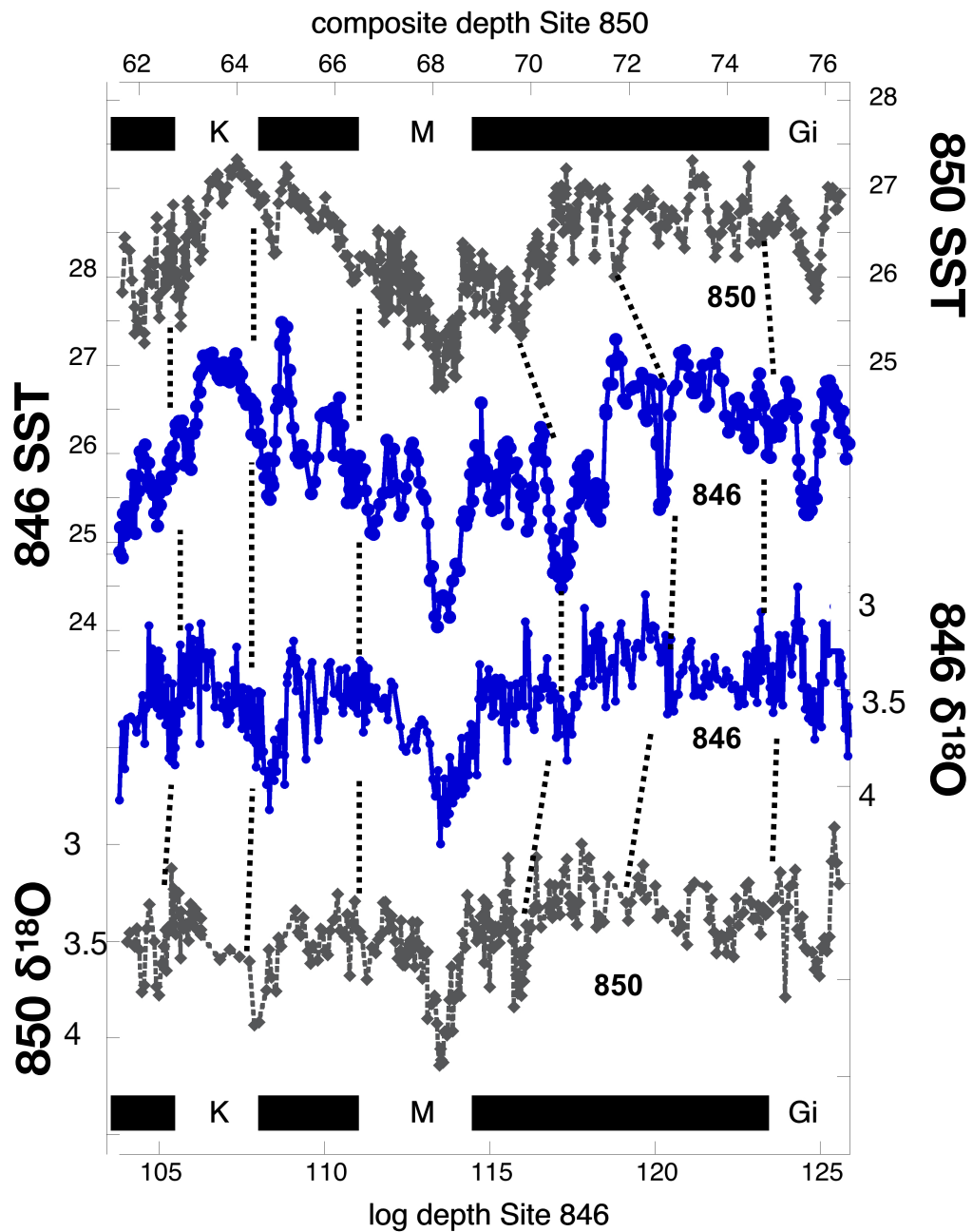
Figure 11. Comparison of the new alkenone-based SST and δ¹⁸O composites from Site 846 to composites from Site 850. The location of magnetic polarity reversals (reversed Kaena, Mammoth and Gilbert polarity zones indicated by abbreviations) at Site 850 can be mapped to Site 846 with high confidence by the close correspondence of SST patterns (note: polarity determinations are only available at Site 850).